Palladium-catalysed Formation of Aroylcobalt Complexes from Iodoarene and Tetracarbonylcobaltate Anion. Syntheses, Characterization and Reactivities of Model Intermediate Complexes†

Yoshihiko Misumi, Youichi Ishii and Masanobu Hidai*
Department of Chemistry and Biotechnology, Faculty of Engineering, The University of Tokyo, Hongo, Tokyo 113, Japan

The complex $[Pd(PPh_3)_4]$ showed good catalytic activity for the formation of aroylcobalt complexes $[Co(OCR)(CO)_3(PPh_3)]$ from RI (R = aryl), $K[Co(CO)_4]$ and PPh_3. Attempts to isolate an intermediate Pd–Co complex in this catalytic reaction were unsuccessful, however a series of heterodinuclear complexes $[(Ph_3P)(OC)RPtCo(CO)_3(PPh_3)]$ (R = Ph **1a**, C_6H_4Me-4 **1b** or Me **1c**), $[(Me_3P)_2(PhCO)PdCo(CO)_4]$ **2** and $[(Me_3P)_2PhPtCo(CO)_4]$ **3** have been prepared from reactions of $[MR(O_3SCF_3)(PR'_3)_2]$ (M = Pt or Pd, R′ = Me or Ph) with $K[Co(CO)_4]$ as model intermediate complexes. Prior to the formation of complex **1**, transient formation of $[(Ph_3P)_2RPtCo(CO)_4]$ was confirmed by ^{31}P NMR spectroscopy of the reaction solution. The reaction of $[PtPh(O_3SCF_3)(PMe_3)_2]$ with $K[Co(CO)_4]$ led to the isolation of the corresponding Pt–Co complex **3**, while the palladium analogue resulted in the formation of the CO insertion product **2**. Crystal structures of compounds **1a**, **1c**, **2** and **3** were determined by X-ray diffraction analyses. Addition of ligands L such as CO, Bu^{t}NC and PMe_3 to **3** in tetrahydrofuran induced heterolytic cleavage of the Pt–Co bond to form $[PtPh(PMe_3)_2L][Co(CO)_4]$. Thermolysis of complexes **1b** and **1c** under CO at 50 °C resulted in reductive elimination of $Co(OCC_6H_4Me\text{-}4)(CO)_3(PPh_3)$ and $Co(OCMe)(CO)_3(PPh_3)$, respectively, from the platinum centre. This strongly suggests the involvement of this type of heterodinuclear Pd–Co complex in the catalytic formation of aroylcobalt complexes.

Homogeneous multimetallic catalyses and their reaction mechanisms are a topic of current interest because several such systems have been found to exhibit unique or enhanced activities.[1] We have long been investigating homogeneous multimetallic catalyses and previously reported that the $[Co_2(CO)_8]$–$[Ru_3(CO)_{12}]$[2] and $[PdCl_2(PPh_3)]$–$[Ru_3(CO)_{12}]$[3] bimetallic systems behave as effective catalysts for carbonylation reactions of olefins and aryl iodides (RI), respectively. More recently, we have found that the $[PdCl_2(PPh_3)_2]$–$[Co_2(CO)_8]$ bimetallic system works effectively for the carbonylation reactions of aryl iodides with CO–$HSiEt_3$ under relatively mild conditions [Scheme 1, equations (1) and (2)].[4,5]

In the course of our studies on the reaction mechanism of these carbonylations we noticed that the transfer of an organic moiety from palladium to cobalt to form an aroylcobalt complex may play an important role in the carbonylation, because the initial activation of RI is considered to be done by a palladium(0) species while the product $R(Et_3SiO)CHCH(OSiEt_3)R$-forming step has been shown to be the hydrosilylation of aroylcobalt complexes $[Co(OCR)(CO)_3(PPh_3)]$ followed by homolytic cleavage of the Co–C bond and coupling of the resulting siloxybenzyl radicals.[5] Actually, we found that the reaction of RI, $[Co(CO)_4]^-$ and PPh_3 is effectively catalysed by a palladium(0) complex to give $[Co(OCR)(CO)_3(PPh_3)]$, and proposed that the catalysis should proceed *via* a Pd–Co heterobimetallic complex.[4] A related Pd-catalysed arylation of some metalate anions, $[Mo(\eta\text{-}C_5H_5)(CO)_3]^-$, $[W(\eta\text{-}C_5H_5)(CO)_3]^-$, $[Mn(CO)_5]^-$ and $[Fe(\eta\text{-}C_5H_5)(CO)_2]^-$ has been reported by Artamkina *et al.*,[6] but no experimental evidence was given with regard to the catalytic mechanism. Now we report the details of the catalytic formation of the aroylcobalt complexes, together with syntheses, characterization and reactivities of some Pd–Co and Pt–Co heterodinuclear complexes as model intermediates.

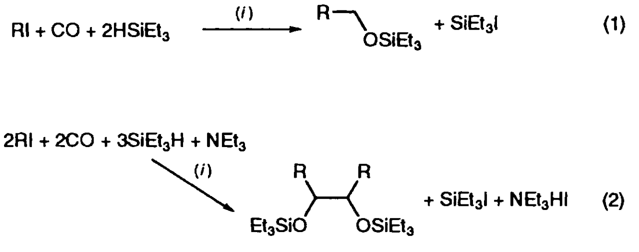

Scheme 1 (i) $[PdCl_2(PPh_3)_2]$, $[Co_2(CO)_8]$

Experimental

General.—All manipulations were carried out under a dry nitrogen atmosphere with standard Schlenk-tube techniques unless otherwise noted. Solvents were dried and distilled under nitrogen by standard methods. Alumina (mesh 70–230, Merck) was used for chromatography. The compounds $[Pd(PPh_3)_4]$,[7] $K[Co(CO)_4]$,[8] $[Pd(C_6H_4Me\text{-}4)I(PPh_3)_2]$,[9] $[PtR(I)(PPh_3)_2]$ (R = Ph or C_6H_4Me-4),[10] $[PtMe(I)(PPh_3)_2]$,[11] $[PdPh(Br)(PMe_3)_2]$[12] and $[PtPh_2(PMe_3)_2]$[13] were prepared according to the literature procedures. Organo-palladium or -platinum triflates $[MR(O_3SCF_3)(phosphine)_2]$ (R = Ph, C_6H_4Me-4 or Me; M = Pd or Pt) were prepared by modifying preparation methods for related palladium or platinum[14,15] complexes. Other reagents were used as obtained from commercial sources. Proton (270 MHz) and ^{31}P-{^1H} (109

---

† *Supplementary data available:* see Instructions for Authors, *J. Chem. Soc., Dalton Trans.*, 1995, Issue 1, pp. xxv–xxx.

MHz) NMR spectra were recorded on a JEOL JNM-EX-270 spectrometer; ^{31}P chemical shifts are reported relative to 85% H_3PO_4. Infrared spectra were recorded on a Shimadzu FTIR-8100M spectrophotometer. Electroconductivities were recorded on a Toa CM-20A digital conductivity meter. Electron-probe microanalyses (EPMA) were performed on a Kevex µX7000 dispersive-type X-ray analyser.

Palladium-catalysed Formation of Aroylcobalt Complexes.—To a solution of $K[Co(CO)_4]$ in tetrahydrofuran (thf) prepared from $[Co_2(CO)_8]$ (141 mg, 0.413 mmol) and an excess of KOH in thf (10 cm^3) was added $[Pd(PPh_3)_4]$ (58 mg, 0.05 mmol) and PPh_3 (144 mg, 0.55 mmol) under a nitrogen atmosphere. The resulting suspension was warmed to 50 °C, RI (0.5 mmol) was added in the dark, and the mixture was stirred at this temperature. The reaction was monitored by checking the conversion of the RI by means of GC. During the reaction precipitation of a white solid (KI, identified by EPMA) was observed. After 3–6 h the mixture was concentrated *in vacuo*, diluted with hexane, and chromatographed on alumina (thf–hexane, 1:2–1:1). The yellow band was collected and dried *in vacuo*. Recrystallization from thf–hexane at -20 °C gave analytically pure $[Co(OCR)(CO)_3(PPh_3)]$ as yellow crystals or a solid.

$[Co(OCPh)(CO)_3(PPh_3)]$ (Found: C, 66.05; H, 4.05. $C_{28}H_{20}CoO_4P$ requires C, 65.90; H, 3.95%): $\tilde{\nu}_{max}/cm^{-1}$ (CO) 2051w, 1975 (sh), 1960s and 1626m (KBr); $\delta_H([^2H_8]thf)$ 6.9–7.9 (m).

$[Co(OCC_6H_4Me\text{-}4)(CO)_3(PPh_3)]$ (Found: C, 66.40; H, 4.35. $C_{29}H_{22}CoO_4P$ requires C, 66.40; H, 4.25%): $\tilde{\nu}_{max}/cm^{-1}$ (CO) 2047w, 1972s, 1954s, 1923 (sh), 1642m and 1619m (KBr); $\delta_H([^2H_8]thf)$ 2.37 (3 H, s), 7.23 (2 H, d, *J* 8.2), 7.51–7.56 (15 H, m) and 7.76 (2 H, d, *J* 8.2 Hz).

$[Co(OCC_6H_4Me\text{-}2)(CO)_3(PPh_3)]$ (Found: C, 66.45; H, 4.30. $C_{29}H_{22}CoO_4P$ requires C, 66.40; H, 4.25%): $\tilde{\nu}_{max}/cm^{-1}$ (CO) 2045w, 1977 (sh), 1966s and 1663m (KBr); $\delta_H([^2H_8]thf)$ 2.35 (3 H, s), 7.10–7.26 (4 H, m) and 7.40–7.53 (15 H, m).

$[Co(C_6H_4Cl\text{-}4)(CO)_3(PPh_3)]$ (Found: C, 61.60; H, 3.50. $C_{28}H_{19}ClCoO_4P$ requires C, 61.75; H, 3.50%): $\tilde{\nu}_{max}/cm^{-1}$(CO) 2049w, 1981s, 1958s, 1925 (sh) and 1628m (KBr); $\delta_H([^2H_8]thf)$ 7.02–7.06 (2 H, m), 7.3–7.8 (15 H, m) and 7.80–7.83 (2 H, m).

$[Co(C_6H_4OMe\text{-}4)(CO)_3(PPh_3)]$ (Found: C, 64.40; H, 4.15. $C_{29}H_{22}CoO_5P$ requires C, 64.45; H, 4.10%): $\tilde{\nu}_{max}/cm^{-1}$ (CO) 2049w, 1979s, 1954s, 1923 (sh), 1638m and 1619m (KBr); $\delta_H([^2H_8]thf)$ 3.85 (3 H, s), 6.95 (2 H, d, *J* 8.9), 7.4–7.8 (15 H, m) and 7.87 (2 H, d, *J* 8.9 Hz).

$[Co(C_6H_4F\text{-}4)(CO)_3(PPh_3)]$ (Found: C, 63.50; H, 3.75. $C_{28}H_{19}CoFO_4P$ requires C, 63.65; H, 3.60%): $\tilde{\nu}_{max}/cm^{-1}$ (CO) 2045w, 1983s, 1966s, 1931 (sh), 1655w, 1630m and 1590m; $\delta_H([^2H_8]thf)$ 7.18 (2 H, pseudo t, *J* 8.8), 7.4–7.6 (15 H, m) and 7.91 [2 H, dd, *J* 8.9 Hz, ^4J(F–H) 5.5 Hz)].

Attempts to Isolate Pd–Co *Dinuclear Complexes with* PPh_3 *Ligands.*—*Method A.* To a suspension of $[Pd(C_6H_4Me\text{-}4)I(PPh_3)_2]$ (0.345 g, 0.386 mmol) in thf (5 cm^3) was added $K[Co(CO)_4]$ (0.39 mmol) in thf (5 cm^3) at room temperature. The reaction mixture gradually turned purple. Addition of PPh_3 (0.202 g, 0.772 mmol) to the mixture caused an immediate change to light yellow. The IR spectrum of the solution showed absorptions at 2047w, 1979s, 1956s and 1644m cm^{-1}, indicating the formation of $[Co(C_6H_4Me\text{-}4)(CO)_3(PPh_3)]$. A white powder of KI and yellow crystals of $[Pd(PPh_3)_4]$ (identified by EPMA) were also recovered from the solution. However, no Pd–Co bimetallic complex was either isolated or confirmed spectroscopically regardless of the addition of PPh_3.

Method B. To a suspension of $[Pd(C_6H_4Me\text{-}4)I(PPh_3)_2]$ (0.343 g, 0.385 mmol) in thf (5 cm^3) was added $Ag(O_3SCF_3)$ (0.099 g, 0.39 mmol) under a carbon monoxide atmosphere. A yellow solid was filtered off, and the filtrate was added to a thf (5 cm^3) solution of $K[Co(CO)_4]$ (0.40 mmol). The reaction mixture immediately turned red. The solvent was removed *in vacuo*, and the residue was extracted with benzene to afford an orange solution, which showed absorptions at 2047w, 1972s, 1954s and 1645m cm^{-1}, indicating the formation of $[Co(C_6H_4Me\text{-}4)(CO)_3(PPh_3)]$. However, no Pd–Co bimetallic complex was isolated from the benzene solution.

Syntheses.—$[(Ph_3P)(OC)RPtCo(CO)_3(PPh_3)]$ **1**. A suspension of $[PtPh(I)(PPh_3)_2]$ (166 mg, 0.18 mmol) in thf (5 cm^3) was treated with $Ag(O_3SCF_3)$ (46.3 mg, 0.18 mmol) at -20 °C to form a colourless solution of $[PtPh(O_3SCF_3)(PPh_3)_2]$ and a precipitate of AgI. The solid was filtered off, and to the filtrate was added a thf solution of $K[Co(CO)_4]$ prepared from $[Co_2(CO)_8]$ (33.8 mg, 0.099 mmol) and an excess of KOH in thf (5 cm^3). The solution immediately became orange. It was stirred for 1 h at room temperature, then evaporated to dryness. The residue was extracted with benzene (5 cm^3) and purified by column chromatography (alumina, benzene). The red fraction was collected, dried *in vacuo* and recrystallized from benzene–hexane to give $[(Ph_3P)(OC)PhPtCo(CO)_3(PPh_3)]$ **1a** (147 mg, 84%) as red crystals (Found: C, 56.95; H, 3.65. $C_{46}H_{35}CoO_4P_2Pt$ requires C, 57.10; H, 3.65%): $\tilde{\nu}_{max}/cm^{-1}$ (CO) 2049s, 1977m, 1925s and 1889s (KBr); $\delta_H(C_6D_6)$ 6.8–7.8 (m); $\delta_P(C_6D_6)$ 18.0 [PtP, ^1J(Pt–P) 2969, ^3J(P–P) 59] and 64.9 [CoP, ^2J(Pt–P) 222, ^3J(P–P) 59 Hz].

The corresponding complexes **1b** (R = $C_6H_4Me\text{-}4$) and **1c** (R = Me) were prepared from $[Pt(C_6H_4Me\text{-}4)I(PPh_3)_2]$ (105 mg, 0.112 mmol) and $[PtMe(I)(PPh_3)_2]$ (96.1 mg, 0.46 mmol) by a similar procedure, in 72 and 32% yield, respectively: **1b** (Found: C, 57.65; H, 3.90. $C_{47}H_{37}CoO_4P_2Pt$ requires C, 57.50; H, 3.80%); $\tilde{\nu}_{max}/cm^{-1}$ (CO) 2047s, 1975m, 1921s and 1887s (KBr); $\delta_H(C_6D_6)$ 2.27 (3 H, s), 6.82 (2 H, d, *J* 7.81), 6.9–7.7 (30 H, m) and 7.54 (2 H, d, *J* 7.81); $\delta_P(C_6D_6)$ 18.6 [PtP, ^1J(Pt–P) 2982, ^3J(P–P) 58] and 66.5 [CoP, ^2J(Pt–P) 223, ^3J(P–P) 58 Hz]; **1c** (Found: C, 55.05; H, 3.85. $C_{41}H_{33}CoO_4P_2Pt$ requires C, 54.35; H, 3.65%); $\tilde{\nu}_{max}/cm^{-1}$ (CO) 2049s, 1972m, 1916s and 1887s (KBr); $\delta_H(C_6D_6)$ 1.56 [3 H, d, ^3J(H–P) 7.2, ^2J(Pt–H) 64.5] and 6.9–8.0 (30 H, m); $\delta_P(C_6D_6)$ 26.3 [PtP, ^1J(Pt–P) 3021, ^3J(P–P) 58] and 67.2 [CoP, ^2J(Pt–P) 222, ^3J(P–P) 56 Hz].

$[(Me_3P)_2(PhCO)PdCo(CO)_4]$ **2**. To a solution of $[PdPh(Br)(PMe_3)_2]$ (191 mg, 0.46 mmol) in thf (10 cm^3) was added $Ag(O_3SCF_3)$ (0.118 mg, 0.46 mmol) at -20 °C under a carbon monoxide atmosphere. The AgBr formed was filtered off, and the pale yellow filtrate allowed to react with a thf solution of $K[Co(CO)_4]$ prepared from $[Co_2(CO)_8]$ (87 mg, 0.25 mmol) and an excess of KOH in thf (5 cm^3). The resulting red solution was stirred for 8 h under a carbon monoxide atmosphere. Then it was evaporated to dryness and the residue extracted with benzene (3 cm^3). The deep red extract was purified by column chromatography (alumina, benzene), and the red fraction was collected, dried *in vacuo*, and recrystallized from benzene–hexane at -20 °C to give $[(Me_3P)_2(PhCO)PdCo(CO)_4]$ **2** (177 mg, 72%) as red crystals. When the reaction was performed under a nitrogen atmosphere the reaction mixture darkened during stirring and the yield of **2** was 40%. Complex **2** (Found: C, 38.30; H, 4.30. $C_{17}H_{23}CoO_5P_2Pd$ requires C, 38.20; H, 4.35%): $\tilde{\nu}_{max}/cm^{-1}$ (CO) 2018s, 1945s, 1914s, 1879s and 1649m (KBr); $\delta_H(C_6D_6)$ 0.87 (18 H, t, *J* 3.5), 7.10–7.18 (3 H, m) and 8.36 (2 H, d, *J* 7.1 Hz); $\delta_P(C_6D_6)$ -23.9 (s).

$[(Me_3P)_2PhPtCo(CO)_4]$ **3**. To a colourless solution of $[PtPh(O_3SCF_3)(PMe_3)_2]$, prepared by treating $[PtPh_2(PMe_3)_2]$ (77.7 mg, 0.155 mmol) in thf (5 cm^3) with CF_3SO_3H (17.3 µl, 0.155 mmol), was added a thf (0.31 cm^3) solution of $K[Co(CO)_4]$ (0.155 mmol). The solution immediately became orange. The solvent was removed to dryness and the residue extracted with benzene (3 cm^3). The extract was purified by column chromatography (alumina, benzene) and recrystallized from benzene–hexane at -20 °C to give $[(Me_3P)_2PhPtCo(CO)_4]$ **3** (59.7 mg, 65%) as red crystals (Found: C, 32.45; H, 4.00. $C_{16}H_{23}CoO_4P_2Pt$ requires C, 32.30; H, 3.90%): $\tilde{\nu}_{max}/cm^{-1}$ (CO) 2016s, 1946s, 1931s and 1850s (KBr); 2020s, 1941s and 1860s (thf); $\delta_H([^2H_8]thf)$ 1.29 [18 H, t, *J* 3.8,

Table 1 Crystallographic data for [$(Ph_3P)(OC)PhPtCo(CO)_3(PPh_3)$] **1a**, [$(Ph_3P)(OC)MePtCo(CO)_3(PPh_3)$] **1c**, [$(Me_3P)_2(PhCO)PdCo(CO)_4$] **2** and [$(Me_3P)_2PhPtCo(CO)_4$] **3***

Complex	**1a**	**1c**	**2**	**3**
Formula	$C_{46}H_{35}CoO_4P_2Pt$	$C_{41}H_{33}CoO_4P_2Pt$	$C_{17}H_{23}CoO_5P_2Pd$	$C_{16}H_{23}CoO_4P_2Pt$
M	967.75	905.68	534.65	595.33
Crystal system	Monoclinic	Triclinic	Monoclinic	Orthorhombic
Space group	$P2_1/c$	$P\bar{1}$	$P2_1/c$	$P2_12_12_1$
a/Å	18.231(2)	13.375(9)	9.7753(8)	12.894(3)
b/Å	10.777(2)	14.687(7)	14.3032(8)	14.121(2)
c/Å	21.043(1)	10.832(9)	16.0758(7)	11.571(2)
α/°		108.64(5)		
β/°	90.338(7)	111.40(6)	92.568(5)	
γ/°		76.40(5)		
U/Å^3	4134.3(8)	1860(2)	2245.4(2)	2106.8(7)
Z	4	2	4	4
D_c/g cm^{-3}	1.555	1.617	1.581	1.877
F(000)	1912	892	1072	1144
Crystal dimensions/mm	0.6 × 0.3 × 0.2	0.5 × 0.3 × 0.2	0.4 × 0.3 × 0.2	0.3 × 0.2 × 0.2
μ/cm^{-1}	39.32	43.13	16.90	75.60
Total data	10 288	8899	5673	2758
Unique data	9985	8535	5371	2758
Observed data [$I > 3\sigma(I)$]	3929	4746	3200	1778
Variables	487	442	235	217
Transmission factor range	0.9989–0.4941	0.9999–0.5750	0.9989–0.9541	0.9989–0.8145
R	0.051	0.051	0.037	0.042
R'	0.025	0.024	0.026	0.028
Goodness of fit	1.85	2.56	2.56	1.51
Largest electron density peak/e Å^{-3}	0.92	1.5	0.49	1.00

* Details in common: $2\theta_{max}$ 55°; scan mode ω–2θ; $R = \Sigma||F_o| - |F_c||/\Sigma|F_o|$; $R' = [\Sigma w(|F_o| - |F_c|)^2/\Sigma wF_o^{\,2}]^{\frac{1}{2}}$.

^3J(Pt–H) 29], 6.87–7.08 (3 H, m) and 7.44 [2 H, d, J 6.8, ^3J(Pt–H) 63]; $\delta_P(C_6D_6)$ −17.9 [^1J(Pt–P) 2670]; δ_P([$^2H_8$]thf) −14.9 [^1J(Pt–P) 2662 Hz].

X-Ray Data Collection and Processing.—Crystals of complexes **1a**, **1c** and **2** suitable for X-ray crystallography were obtained by slow diffusion of hexane into corresponding benzene solutions of the complexes, while those of **3** were obtained by cooling its benzene–hexane (1:5) solution to −20 °C. In each case a suitable crystal was sealed in a glass capillary under nitrogen. All the measurements were made on a Rigaku AFC7R diffractometer at 20 °C by using graphite-monochromated Mo-Kα radiation (λ 0.710 69 Å). Crystallographic and experimental details are summarized in Table 1. Unit-cell parameters were determined from the least-squares refinement of 25 centred reflections in the ranges $37.0 < 2\theta < 39.5°$ for **1a**, $38.3 < 2\theta < 39.3°$ for **1c**, $38.0 < 2\theta < 39.8°$ for **2** and $20.2 < 2\theta < 28.6°$ for **3**. Intensity data were processed[16] and corrected for Lorentz-polarization effects and absorption by the empirical ψ-scan method. A decay correction (−3.84%) was applied for **1c**, but the other complexes showed no appreciable decay during the data collection. The structures were solved by heavy-atom Patterson methods and expanded using Fourier techniques. All non-hydrogen atoms were refined anisotropically. The coordinates of all hydrogen atoms were calculated at ideal positions (C–H 0.95 Å) and were not refined. For **3** the coordinates of all atoms were inverted and the complete structure was refined again. In this case the final residuals were $R = 0.057$ and $R' = 0.043$, which are significantly higher than those for the first enantiomorph; thus, the latter was deemed to be correct. The structures were depicted with the ORTEP II software.[17]

Additional material available from the Cambridge Crystallographic Data Centre comprises H-atom coordinates, thermal parameters and remaining bond lengths and angles.

Reactions of Complex **3**.—When Bu^{t}NC (0.4 mg, 5 μmol) was added to a thf solution of complex **3** (3 mg, 5 μmol) the red colour of the solution immediately disappeared. In the IR spectrum of the resulting mixture (NaCl cell) the carbonyl absorptions due to **3** were absent, and strong absorptions attributable to [$Co(CO)_4$]$^-$ (1888 cm^{-1}) and [$PtPh(PMe_3)_2(CNBu^t)$]$^+$ (2197 cm^{-1}) were observed. No other carbonyl absorption was detected.

Similar reaction mixtures from separate runs were also analysed by ^{31}P-{^{1}H} NMR (in [$^2H_8$]thf) and electroconductivity measurements (in thf). Reactions of complex **3** with PMe_3 (1 mol dm^{-3} solution in thf) or CO (1 atm, *ca.* 10^5 Pa) were performed and analysed similarly.

Thermolysis Reactions of the Heterodinuclear Complexes.—In a typical run, complex **1b** (7.7 mg, 7.8 μmol) was dissolved in C_6D_6 (0.5 cm^3) and the solution was stirred at 50 °C under a carbon monoxide atmosphere for 2 h. After cooling to room temperature, the resulting solution was transferred to an NMR tube and the ^{1}H spectrum recorded, which indicated the formation of [$Co(C_6H_4Me\text{-}4)(CO)_3(PPh_3)$] in 47% yield. The IR spectrum of the solution showed absorptions at 2049w, 1981s, 1956s and 1645m cm^{-1}, which also confirmed this formulation.

Results and Discussion

Palladium-catalysed Formation of [$Co(OCR)(CO)_3(PPh_3)$] *from* RI, K[$Co(CO)_4$] *and* PPh_3.—Tetracarbonylcobaltate(−1) anion [$Co(CO)_4$]$^-$ is known to react with alkyl halides or acid halides to form acylcobalt complexes.[18] Although the nucleophilicity of this anion is one of the lowest among those of carbonylmetalate anions,[19] the reactions with such substrates usually proceed below 0 °C. However, [$Co(CO)_4$]$^-$ does not react with aryl halides. For example, no reaction was observed with 4-MeC_6H_4I in thf even at 50 °C. We have now found that the reactions between [$Co(CO)_4$]$^-$ and aryl halides are effectively promoted by addition of [$Pd(PPh_3)_4$]. Thus, when [$Co(CO)_4$]$^-$ was allowed to react with 4-MeC_6H_4I and an equimolar amount of PPh_3 in the presence of 10 mol% of [$Pd(PPh_3)_4$], the solution turned yellow and white precipitate identified as KI by EPMA gradually formed. The complex

Table 2 Formation of aroylcobalt complexes catalysed by $[Pd(PPh_3)_4]$

R	Reaction time/h	Conversion[a] (%)	Yield[b] (%)
Ph	4	98	73
C_6H_4Me-4	4	100	79
C_6H_4Me-2	6	75	32
C_6H_4Cl-4	4	98	68
C_6H_4OMe-4	4	100	81
C_6H_4F-4	6	93	36

[a] Based on the starting iodoarene and determined by GLC. [b] Isolated yield.

$[Co(C_6H_4Me\text{-}4)(CO)_3(PPh_3)]$ was isolated from the reaction mixture after purification by column chromatography. The results of reactions between $[Co(CO)_4]^-$ and several RI are summarized in Table 2. The reactions with RI (R = Ph, 4-MeC_6H_4, 4-ClC_6H_4 or 4-$MeOC_6H_4$) proceeded smoothly and were completed within 3–4 h, but in the case of R = 2-MeC_6H_4 and 4-FC_6H_4 were rather slow and $[Co(C_6H_4Me\text{-}2)(CO)_3(PPh_3)]$ and $[Co(C_6H_4F\text{-}4)(CO)_3(PPh_3)]$ were obtained in only 32 and 36% yield, respectively, after 6 h.

This Pd-catalysed reaction provides a convenient route to aroylcobalt complexes from RI. Although it ends in the formation of a C–Co bond and corresponds to formal activation of RI with $[Co(CO)_4]^-$, the initial activation of RI and the introduction of the organic group onto the cobalt centre is presumed to be conducted by the action of a palladium species. A Pd–Co bimetallic intermediate complex may be formed during the reaction. Further, it should be pointed out that this process is actually involved and plays a key role in the bimetallically catalysed reaction.[5]

Synthesis and Structure of $[(Ph_3P)(OC)RPtCo(CO)_3(PPh_3)]$ **1**.—In order to shed light upon the bimetallic interaction during the aroylcobalt complex formation, we embarked on the synthesis of model intermediate complexes. Previously, Komiya and co-workers[20] reported that several Pt–Mo or Pt–W dinuclear complexes having an alkyl or aryl ligand on the platinum centre undergo reductive-elimination reactions from the platinum centre to form the corresponding alkyl- or aryl-molybdenum or -tungsten complexes. In the present Pd-catalysed formation of aroylcobalt complexes it is also reasonable to assume that a Pd–Co dinuclear intermediate should first be formed, and the succeeding reductive elimination from the palladium centre accompanied by the insertion of CO results in the production of aroylcobalt complexes. Therefore, we at first examined stoichiometric reactions of $[Pd(C_6H_4Me\text{-}4)I(PPh_3)_2]$ (under nitrogen) or $[Pd(C_6H_4Me\text{-}4)(O_3SCF_3)(PPh_3)_2]$ (under CO) with $K[Co(CO)_4]$, but in all cases the only isolable product was $[Co(OCC_6H_4Me\text{-}4)(CO)_3(PPh_3)]$ and no identifiable Pd–Co bimetallic complex was obtained. This is probably due to the facile reductive elimination of aryl- or aroyl-cobalt species from the palladium centre.

In order to stabilize the bimetallic species, we tried to use the corresponding organoplatinum instead of the organopalladium complexes, because platinum complexes are known to have a lower tendency to undergo reductive-elimination reactions in comparison with the palladium analogues.[21] The complex $[Pt(C_6H_4Me\text{-}4)I(PPh_3)_2]$ did not react with $K[Co(CO)_4]$ in thf even at 50 °C. In contrast, $[PtR(O_3SCF_3)(PPh_3)_2]$ readily reacted with $[Co(CO)_4]^-$ in thf at room temperature, and a series of stable dinuclear complexes $[(Ph_3P)(OC)RPtCo(CO)_3(PPh_3)]$ (R = Ph **1a**, C_6H_4Me-4 **1b** or Me **1c**) were isolated after column chromatography and recrystallization.

The $^{31}P\text{-}\{^1H\}$ NMR spectra of complexes **1** exhibited two distinct doublet signals [^3J(P–P) *ca.* 60 Hz] due to co-ordinated PPh_3. The upper-field signals were accompanied by satellites with large coupling constants characteristic of platinum–phosphine complexes [^1J(Pt–P) *ca.* 2980 Hz], while the satellites of the broad lower-field signals showed much smaller coupling constants [^2J(Pt–P) *ca.* 220 Hz]. This clearly indicates that one of the two PPh_3 ligands originally co-ordinated by the platinum atom has migrated to the cobalt centre in **1**.

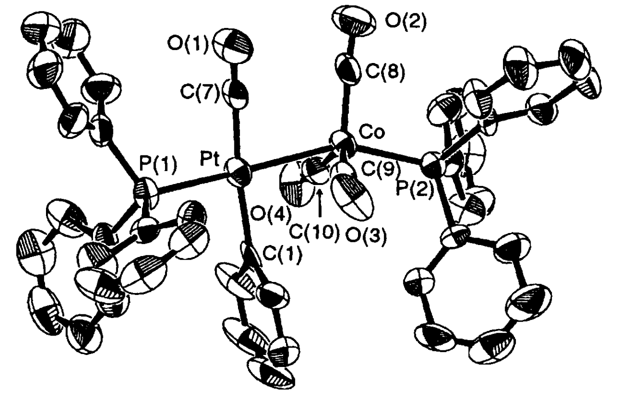

Fig. 1 An ORTEP drawing for complex **1a** drawn at the 50% probability level

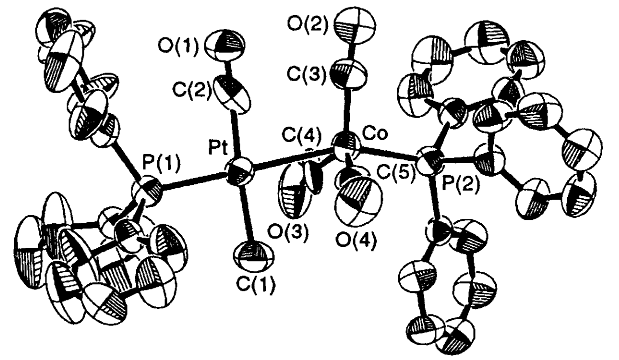

Fig. 2 An ORTEP drawing for complex **1c** drawn at the 50% probability level

The molecular structures of complexes **1a** and **1c** were confirmed by X-ray analysis. The atomic coordinates are listed in Tables 3 and 4, ORTEP drawings are depicted in Figs. 1 and 2 and selected bond distances and angles are listed in Tables 5 and 6. In full agreement with the $^{31}P\text{-}\{^1H\}$ NMR, one of the PPh_3 ligands is co-ordinated to the cobalt atom, and in compensation for this one of the CO ligands has migrated to the platinum centre from the cobalt. The co-ordination around the platinum atom is square planar, the cobalt atom and the PPh_3 ligand [P(1)] being mutually *trans*. The phenyl or methyl ligand in **1a** or **1c**, respectively, occupies the position *cis* to the cobalt. The cobalt atom has distorted trigonal-bypyramidal geometry, the platinum atom and the PPh_3 ligand [P(2)] occupying the apical positions [Pt–Co–P(2) 152.1(1)° in **1a** and 155.28(9)° in **1c**]. The Pt–Co distances [2.645(2) Å in **1a** and 2.658(2) Å in **1c**] are within the reported range[22] of Pt–Co distances, but rather shorter than that of **3** (see below). One of the carbonyl ligands on the cobalt atom in **1a** or **1c** is located close to the platinum [Pt···C(9) 2.58(1) Å in **1a**, Pt···C(4) 2.49(2) Å in **1c**]. These carbonyls may be classified as linear semibridging on the basis of the Pt–Co–C and Co–C–O angles [Pt–Co–C(9) 68.2(4) and Co–C(9)–O(3) 170(1)° in **1a**; Pt–Co–C(4) 66.1(5) and Co–C(4)–O(3) 169(1)° in **1c**].[23]

Previously, Braunstein and co-workers[14] reported the formation of a thermally unstable complex *trans*-$[(Ph_3P)_2MePtCo(CO)_4]$ on the basis of low-temperature ^{31}P NMR measurements of a reaction mixture containing $[PtMe(OClO_3)(PPh_3)_2]$ and $[Co(CO)_4]^-$, but they did not refer to the ligand migration shown above. We monitored the reaction of $[Pt(C_6H_4Me\text{-}4)(O_3SCF_3)(PPh_3)_2]$ with $K[Co(CO)_4]$ in $[^2H_8]$-thf by means of $^{31}P\text{-}\{^1H\}$ NMR spectroscopy. In an early stage

Table 3 Positional parameters for [(Ph$_3$P)(OC)PhPtCo(CO)$_3$(PPh$_3$)] **1a**

Atom	*x*	*y*	*z*
Pt	0.199 08(3)	0.038 59(5)	−0.214 18(3)
Co	0.272 48(9)	0.113 1(1)	−0.315 28(7)
P(1)	0.134 9(1)	−0.020 9(3)	−0.126 1(1)
P(2)	0.358 5(2)	0.090 8(3)	−0.385 8(1)
O(1)	0.166 1(5)	0.312 1(7)	−0.204 5(4)
O(2)	0.234 0(5)	0.367 9(7)	−0.345 6(4)
O(3)	0.378 0(4)	0.071 0(8)	−0.212 1(4)
O(4)	0.164 9(4)	−0.047 2(8)	−0.380 4(4)
C(1)	0.232 6(7)	−0.142(1)	−0.225 2(6)
C(2)	0.189 0(8)	−0.227(1)	−0.261 4(6)
C(3)	0.213(1)	−0.346(1)	−0.272 0(7)
C(4)	0.278(1)	−0.388(1)	−0.244 2(8)
C(5)	0.319 6(7)	−0.308(1)	−0.207 3(7)
C(6)	0.295 9(7)	−0.190(1)	−0.197 3(5)
C(7)	0.178 3(7)	0.207(1)	−0.209 8(6)
C(8)	0.248 1(6)	0.267(1)	−0.331 8(5)
C(9)	0.331 6(6)	0.085(1)	−0.249 3(6)
C(10)	0.209 7(6)	0.012(1)	−0.354 9(5)
C(11)	0.073 9(6)	0.102(1)	−0.097 2(6)
C(12)	0.030 5(8)	0.162(1)	−0.141 3(6)
C(13)	−0.012 8(8)	0.261(2)	−0.122 1(8)
C(14)	−0.011 4(9)	0.301(1)	−0.059 7(9)
C(15)	0.036 1(8)	0.242(1)	−0.018 5(6)
C(16)	0.078 3(6)	0.142(1)	−0.035 0(6)
C(17)	0.195 0(6)	−0.056(1)	−0.057 3(5)
C(18)	0.262 4(6)	0.004(1)	−0.054 7(5)
C(19)	0.306 0(6)	−0.012(1)	0.000 2(6)
C(20)	0.283 1(8)	−0.088(1)	0.047 3(6)
C(21)	0.218 0(9)	−0.146(1)	0.041 8(6)
C(22)	0.169 6(6)	−0.131(1)	−0.009 2(6)
C(23)	0.079 3(7)	−0.158(1)	−0.135 5(5)
C(24)	0.005 0(9)	−0.148(1)	−0.151 9(6)
C(25)	−0.039 6(8)	−0.252(2)	−0.163 6(7)
C(26)	−0.007 7(9)	−0.365(1)	−0.160 5(7)
C(27)	0.067 0(9)	−0.378(1)	−0.143 5(7)
C(28)	0.107 6(6)	−0.275(1)	−0.131 7(6)
C(29)	0.419 9(5)	0.221(1)	−0.394 6(6)
C(30)	0.452 0(6)	0.248(1)	−0.452 1(6)
C(31)	0.504 8(7)	0.343(1)	−0.457 0(6)
C(32)	0.524 8(7)	0.410(1)	−0.403 0(8)
C(33)	0.489 6(8)	0.386(1)	−0.348 3(7)
C(34)	0.438 3(7)	0.292(1)	−0.343 2(6)
C(35)	0.323 0(5)	0.061(1)	−0.465 2(5)
C(36)	0.334 2(6)	−0.049(1)	−0.496 7(5)
C(37)	0.300 7(7)	−0.071(1)	−0.553 5(7)
C(38)	0.257 2(6)	0.017(2)	−0.580 8(6)
C(39)	0.246 2(6)	0.129(1)	−0.551 3(6)
C(40)	0.278 9(6)	0.149(1)	−0.493 7(6)
C(41)	0.420 1(6)	−0.038(1)	−0.371 5(5)
C(42)	0.395 8(7)	−0.148(1)	−0.348 5(7)
C(43)	0.440 4(10)	−0.248(1)	−0.340 1(6)
C(44)	0.516 0(10)	−0.236(1)	−0.352 7(7)
C(45)	0.541 9(8)	−0.127(2)	−0.374 2(8)
C(46)	0.496 1(7)	−0.030(1)	−0.384 6(5)

Table 4 Positional parameters for [(Ph$_3$P)(OC)MePtCo(CO)$_3$(PPh$_3$)] **1c**

Atom	*x*	*y*	*z*
Pt	0.185 44(3)	0.194 73(3)	−0.261 33(4)
Co	0.324 1(1)	0.238 66(9)	−0.350 7(1)
P(1)	0.073 2(2)	0.161 0(2)	−0.173 0(2)
P(2)	0.393 1(2)	0.333 3(2)	−0.407 3(2)
O(1)	0.371 0(5)	0.044 9(4)	−0.166 5(6)
O(2)	0.507 5(5)	0.088 2(5)	−0.318 4(7)
O(3)	0.298 5(8)	0.386 1(6)	−0.115 4(8)
O(4)	0.157 8(6)	0.177 6(6)	−0.610 8(7)
C(1)	0.061 4(7)	0.296 0(6)	−0.336 4(9)
C(2)	0.301 0(7)	0.104 2(7)	−0.203 6(9)
C(3)	0.431 6(7)	0.148 3(8)	−0.326 8(10)
C(4)	0.304(1)	0.316(1)	−0.217(1)
C(5)	0.224 5(7)	0.204 0(7)	−0.502(1)
C(6)	0.126 3(7)	0.056 9(7)	−0.104 9(10)
C(7)	0.094 2(10)	−0.031 2(8)	−0.176 4(10)
C(8)	0.150(2)	−0.115(1)	−0.132(1)
C(9)	0.231(1)	−0.105(1)	−0.014(2)
C(10)	0.262(1)	−0.019(1)	0.063(2)
C(11)	0.208 9(9)	0.062 1(7)	0.015(1)
C(12)	−0.057 6(7)	0.137 1(6)	−0.285 6(9)
C(13)	−0.079 9(8)	0.120 7(8)	−0.422(1)
C(14)	−0.181(1)	0.098 6(8)	−0.514 9(9)
C(15)	−0.259 8(8)	0.092 2(7)	−0.472(1)
C(16)	−0.238 3(10)	0.110(1)	−0.338(1)
C(17)	−0.139 2(9)	0.133 5(10)	−0.247 0(9)
C(18)	0.050 5(7)	0.258 5(6)	−0.025 5(9)
C(19)	0.083 2(8)	0.347 2(9)	0.007(1)
C(20)	0.065 9(10)	0.420 7(8)	0.119(1)
C(21)	0.016 6(9)	0.407 7(8)	0.194 4(10)
C(22)	−0.012(1)	0.321(1)	0.169(1)
C(23)	0.006(1)	0.247 9(8)	0.060(1)
C(24)	0.321 1(7)	0.458 8(6)	−0.393 3(8)
C(25)	0.374 7(7)	0.538 4(7)	−0.337 1(9)
C(26)	0.314 9(9)	0.630 1(7)	−0.335 2(9)
C(27)	0.204 2(9)	0.642 3(6)	−0.389 3(9)
C(28)	0.151 2(7)	0.561 3(7)	−0.443 5(9)
C(29)	0.209 5(7)	0.470 4(6)	−0.443 8(8)
C(30)	0.399 7(6)	0.297 0(6)	−0.582 8(8)
C(31)	0.437 3(7)	0.203 6(7)	−0.636 4(10)
C(32)	0.451 6(8)	0.174 1(7)	−0.765(1)
C(33)	0.424 9(8)	0.239 1(8)	−0.841 0(9)
C(34)	0.382 9(8)	0.331 9(8)	−0.793 2(10)
C(35)	0.370 8(7)	0.360 5(6)	−0.664 7(10)
C(36)	0.531 2(6)	0.353 9(5)	−0.304 2(9)
C(37)	0.564 3(8)	0.365 8(7)	−0.164(1)
C(38)	0.667 5(10)	0.385 6(7)	−0.081 9(9)
C(39)	0.740 1(8)	0.394 6(8)	−0.137(1)
C(40)	0.709 3(9)	0.383 2(7)	−0.275(1)
C(41)	0.605 4(8)	0.364 1(6)	−0.356 6(9)

of the reaction, an intermediate species showing a single ^{31}P NMR signal [δ 22.0, ^1J(Pt–P) 3018 Hz] was observed, which can be assigned to *trans*-[(Ph$_3$P)$_2$(4-MeC$_6$H$_4$)PtCo(CO)$_4$]. On standing at room temperature this species gradually disappeared and a set of ^{31}P signals due to **1b** emerged. It is clear that the first Pt–Co bond formation between [PtR(O$_3$SCF$_3$)(PPh$_3$)$_2$] and [Co(CO)$_4$]$^-$ gives *trans*-[(Ph$_3$P)$_2$RPtCo(CO)$_4$], but the succeeding migration of a PPh$_3$ ligand from the platinum to the cobalt and the concurrent migration of a CO ligand from the cobalt to the platinum result in the production of complex **1** as the thermodynamically stable final product. During this migration process, the alkyl or aryl group slips to the position *cis* to the cobalt atom. Probably the ligand reorientation is caused by the steric congestion between the ligands on the dinuclear centre, because no such reaction was observed in the cases of the less sterically demanding PMe$_3$ complexes **2** and **3** (see below).

Synthesis and Structure of [(Me$_3$P)$_2$(PhCO)PdCo(CO)$_4$] **2**.—With the intention of stabilizing the bimetallic model complexes, we also used phenyl-palladium and -platinum complexes with PMe$_3$ ligands. When the reaction of [PdPh(O$_3$SCF$_3$)(PMe$_3$)$_2$] with K[Co(CO)$_4$] was performed under a nitrogen atmosphere a dinuclear benzoyl complex

Table 5 Selected bond distances (Å), non-bonding contacts (Å) and angles (°) for complex **1a**

Pt–Co	2.645(2)	Co–C(8)	1.76(1)
Pt–P(1)	2.289(3)	Co–C(9)	1.78(1)
Pt–C(1)	2.05(1)	Co–C(10)	1.78(1)
Pt–C(7)	1.86(1)	Pt · · · C(9)	2.58(1)
Co–P(2)	2.179(3)		
Co–Pt–P(1)	178.6(1)	P(2)–Co–C(8)	98.8(4)
Co–Pt–C(1)	92.6(3)	P(2)–Co–C(9)	94.5(4)
Co–Pt–C(7)	81.2(3)	P(2)–Co–C(10)	94.4(4)
P(1)–Pt–C(1)	88.8(3)	C(8)–Co–C(9)	117.7(5)
P(1)–Pt–C(7)	97.4(4)	C(8)–Co–C(10)	109.0(5)
C(1)–Pt–C(7)	173.3(5)	C(9)–Co–C(10)	130.3(5)
Pt–Co–P(2)	152.1(1)	Pt–C(7)–O(1)	177(1)
Pt–Co–C(8)	108.5(4)	Co–C(8)–O(2)	176(1)
Pt–Co–C(9)	68.2(4)	Co–C(9)–O(3)	170(1)
Pt–Co–C(10)	82.2(4)	Co–C(10)–O(4)	174(1)

Table 6 Selected bond distances (Å), non-bonding contacts (Å) and angles (°) for complex **1c**

Pt–Co	2.658(2)	Co–C(3)	1.716(9)
Pt–P(1)	2.261(2)	Co–C(4)	1.59(2)
Pt–C(1)	2.062(8)	Co–C(5)	1.71(1)
Pt–C(2)	1.846(10)	Pt · · · C(4)	2.49(2)
Co–P(2)	2.173(2)		
Co–Pt–P(1)	176.75(8)	P(2)–Co–C(3)	99.8(3)
Co–Pt–C(1)	93.6(2)	P(2)–Co–C(4)	95.8(5)
Co–Pt–C(2)	82.5(3)	P(2)–Co–C(5)	99.1(3)
P(1)–Pt–C(1)	87.6(2)	C(3)–Co–C(4)	117.6(6)
P(1)–Pt–C(2)	96.4(3)	C(3)–Co–C(5)	111.8(5)
C(1)–Pt–C(2)	175.7(4)	C(4)–Co–C(5)	124.6(6)
Pt–Co–P(2)	155.28(9)	Pt–C(2)–O(1)	177.0(9)
Pt–Co–C(3)	103.5(3)	Co–C(3)–O(2)	174.5(9)
Pt–Co–C(4)	66.1(5)	Co–C(4)–O(3)	169(1)
Pt–Co–C(5)	79.7(3)	Co–C(5)–O(4)	177(1)

Table 7 Positional parameters for $[(Me_3P)_2(PhCO)PdCo(CO)_4]$ **2**

Atom	*x*	*y*	*z*
Pd	0.270 42(4)	0.221 66(3)	−0.139 12(2)
Co	0.552 66(6)	0.209 14(6)	−0.108 92(4)
P(1)	0.265 4(2)	0.381 0(1)	−0.109 3(1)
P(2)	0.237 2(1)	0.061 8(1)	−0.161 6(1)
O(1)	−0.012 4(3)	0.226 0(3)	−0.111 7(2)
O(2)	0.483 9(4)	0.226 0(5)	−0.284 9(3)
O(3)	0.400 6(4)	0.170 8(3)	0.039 6(2)
O(4)	0.722 4(5)	0.370 9(3)	−0.067 6(3)
O(5)	0.737 9(4)	0.052 1(3)	−0.111 0(3)
C(1)	0.068 0(4)	0.231 7(3)	−0.166 0(3)
C(2)	0.018 3(4)	0.244 0(3)	−0.255 1(3)
C(3)	0.107 2(4)	0.263 0(3)	−0.318 0(3)
C(4)	0.056 8(5)	0.271 4(4)	−0.399 3(3)
C(5)	−0.080 0(5)	0.259 0(4)	−0.418 3(3)
C(6)	−0.167 2(5)	0.239 5(4)	−0.356 8(3)
C(7)	−0.119 4(4)	0.232 7(3)	−0.276 1(3)
C(8)	0.501 7(5)	0.219 2(5)	−0.214 2(4)
C(9)	0.453 6(5)	0.188 1(4)	−0.022 1(4)
C(10)	0.653 7(6)	0.308 3(4)	−0.084 1(4)
C(11)	0.663 9(6)	0.112 9(4)	−0.110 6(4)
C(12)	0.334 2(7)	0.408 8(5)	−0.005 9(5)
C(13)	0.361 8(8)	0.453 5(5)	−0.173 7(5)
C(14)	0.101 8(7)	0.438 5(4)	−0.107 8(6)
C(15)	0.358 9(7)	−0.018 6(4)	−0.120 6(5)
C(16)	0.227(1)	0.027 4(6)	−0.267 1(6)
C(17)	0.085 5(8)	0.015 6(5)	−0.128 0(9)

Table 8 Selected bond distances (Å), non-bonding contacts (Å) and angles (°) for complex **2**

Pd–Co	2.7856(7)	Co–C(10)	1.764(6)
Pd–P(1)	2.330(2)	Co–C(11)	1.756(6)
Pd–P(2)	2.336(2)	C(1)–O(1)	1.204(4)
Pd–C(1)	2.012(4)	C(1)–C(2)	1.502(6)
Co–C(8)	1.748(6)	Pd · · · C(8)	2.610(5)
Co–C(9)	1.760(6)	Pd · · · C(9)	2.584(5)
Co–Pd–P(1)	93.26(4)	C(8)–Co–C(11)	101.5(3)
Co–Pd–P(2)	95.38(4)	C(9)–Co–C(10)	106.3(3)
Co–Pd–C(1)	177.6(1)	C(9)–Co–C(11)	104.0(3)
P(1)–Pd–P(2)	170.24(6)	C(10)–Co–C(11)	107.1(2)
P(1)–Pd–C(1)	86.8(1)	Pd–C(1)–O(1)	120.5(3)
P(2)–Pd–C(1)	84.7(1)	Pd–C(1)–C(2)	119.1(3)
Pd–Co–C(8)	65.7(2)	O(1)–C(1)–C(2)	120.4(4)
Pd–Co–C(9)	64.8(2)	Co–C(8)–O(2)	172.2(5)
Pd–Co–C(10)	121.9(2)	Co–C(9)–O(3)	172.9(5)
Pd–Co–C(11)	131.1(2)	Co–C(10)–O(4)	178.0(6)
C(8)–Co–C(9)	129.7(2)	Co–C(11)–O(5)	178.4(6)
C(8)–Co–C(10)	106.6(3)		

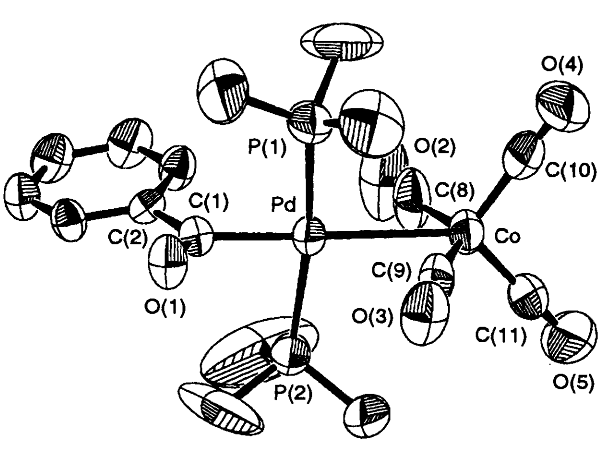

Fig. 3 An ORTEP drawing for complex **2** drawn at the 50% probability level

$[(Me_3P)_2(PhCO)PdCo(CO)_4]$ **2** was isolated in low yield (40%). A similar reaction under CO improved the yield to 72%. The IR spectrum of **2** shows a ν(CO) band at 1649 cm^{-1} due to the benzoyl group. In the ^1H NMR spectrum the signal of PMe_3 appears as a virtual triplet (*J* 3.5 Hz) characteristic of two *trans* PMe_3 ligands, and this is in accordance with the $^{31}P-\{^1H\}$ NMR spectrum which exhibits only one singlet. These spectroscopic data as well as the analytical data fully support the formulation of **2**, which was further confirmed by X-ray analysis.

The atomic coordinates for complex **2** are listed in Table 7, an ORTEP drawing is given in Fig. 3 and selected bond distances and angles are listed in Table 8. The co-ordination around the palladium atom is square planar, where the cobalt atom and the benzoyl ligand are mutually *trans*. The $Co(CO)_4$ moiety can be regarded as distorted tetrahedral, and the Pd–Co bond bisects the largest C(8)–Co–C(9) angle. The Pd–Co distance [2.7856(7) Å] is considerably longer than that of a structurally related complex $[(PhHNN{=}CMeC_6H_4)Pd(py)Co(CO)_4]$ (py = pyridine) [2.604(1) Å][24] probably due to the stronger *trans* influence of the benzoyl group than that of the nitrogen atom of the hydrazone ligand. Two of the carbonyl ligands on the cobalt atom are located close to the palladium [Pd · · · C(8) 2.610(5), Pd · · · C(9) 2.584(5) Å]. Judging from the Pd–Co–C and Co–C–O angles [Pd–Co–C(8) 65.7(2), Pd–Co–C(9) 64.8(2), Co–C(8)–O(2) 172.2(5) and Co–C(9)–O(3) 172.9(5)°], C(8)–O(2) and C(9)–O(3) are linear semibridging and their interactions with the palladium are weak.[23]

Synthesis and Structure of $[(Me_3P)_2PhPtCo(CO)_4]$ **3**.—The reaction of $[PtPh(O_3SCF_3)(PMe_3)_2]$, prepared from $[PtPh_2(PMe_3)_2]$ and CF_3SO_3H in thf, with $K[Co(CO)_4]$ under

Table 9 Positional parameters for [(Me$_3$P)$_2$PhPtCo(CO)$_4$] **3**

Atom	*x*	*y*	*z*
Pt	−0.029 87(5)	0.013 72(4)	−0.028 09(5)
Co	0.176 4(2)	0.050 1(2)	−0.039 4(3)
P(1)	−0.011 4(4)	−0.122 4(3)	0.080 9(4)
P(2)	−0.066 5(3)	0.154 2(3)	−0.123 0(4)
O(1)	0.109(1)	0.129(1)	0.187(1)
O(2)	0.099(1)	−0.070 8(8)	−0.221 8(9)
O(3)	0.354(1)	−0.063 7(10)	0.022(2)
O(4)	0.264(1)	0.202(1)	−0.178(1)
C(1)	−0.184 7(9)	0.013(1)	0.016(2)
C(2)	−0.219(1)	0.061(1)	0.119(2)
C(3)	−0.322(2)	0.069(2)	0.151(2)
C(4)	−0.387(2)	0.026(2)	0.083(2)
C(5)	−0.363(1)	−0.032(1)	−0.022(3)
C(6)	−0.256(1)	−0.036(1)	−0.055(2)
C(7)	0.132(1)	0.101(1)	0.102(2)
C(8)	0.115(1)	−0.023(1)	−0.152(1)
C(9)	0.285(1)	−0.020(2)	−0.002(2)
C(10)	0.225(1)	0.145(1)	−0.124(2)
C(11)	−0.014(2)	−0.099(1)	0.234(1)
C(12)	−0.114(1)	−0.209(1)	0.066(2)
C(13)	0.104(1)	−0.195(1)	0.063(2)
C(14)	−0.037(1)	0.255 9(9)	−0.037(1)
C(15)	−0.201(1)	0.172(1)	−0.167(2)
C(16)	−0.004(1)	0.179(1)	−0.258(1)

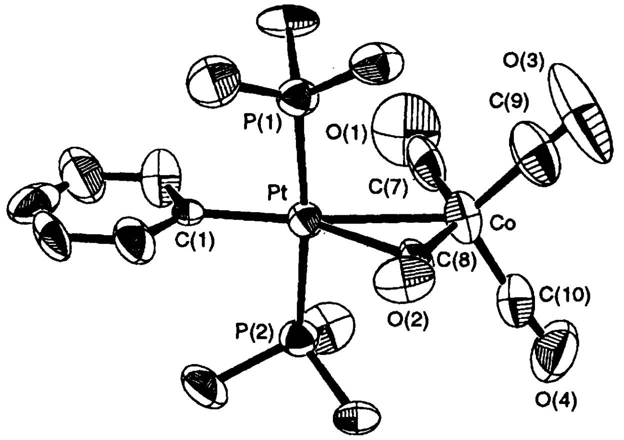

Fig. 4 An ORTEP drawing for complex **3** drawn at the 50% probability level

a nitrogen atmosphere gave a Pt–Co dinuclear complex [(Me$_3$P)$_2$PhPtCo(CO)$_4$] **3** in 65% yield after purification by column chromatography and recrystallization. Spectroscopic analysis clearly indicated that the PMe$_3$ ligands occupy the *trans* positions around the platinum centre, the phenyl ligand remained unchanged in contrast to the case of **2**.

Table 10 Selected bond distances (Å) and angles (°) for complex **3**

Pt–Co	2.711(2)	Co–C(7)	1.88(2)
Pt–P(1)	2.312(4)	Co–C(8)	1.84(2)
Pt–P(2)	2.317(4)	Co–C(9)	1.77(2)
Pt–C(1)	2.06(1)	Co–C(10)	1.78(2)
Pt–C(8)	2.41(1)		
Co–Pt–P(1)	94.7(1)	Pt–Co–C(10)	121.2(6)
Co–Pt–P(2)	90.9(1)	C(7)–Co–C(8)	134.6(7)
Co–Pt–C(1)	164.3(5)	C(7)–Co–C(9)	104.0(10)
Co–Pt–C(8)	41.7(4)	C(7)–Co–C(10)	107.4(9)
P(1)–Pt–P(2)	172.8(2)	C(8)–Co–C(9)	101.6(8)
P(1)–Pt–C(1)	87.7(4)	C(8)–Co–C(10)	100.7(8)
P(1)–Pt–C(8)	93.7(4)	C(9)–Co–C(10)	105.9(10)
P(2)–Pt–C(1)	85.7(4)	Pt–C(8)–O(2)	115(10)
P(2)–Pt–C(8)	93.6(4)	Co–C(7)–O(1)	177(2)
C(1)–Pt–C(8)	153.8(6)	Co–C(8)–O(2)	165(1)
Pt–Co–C(7)	74.7(5)	Co–C(9)–O(3)	179(2)
Pt–Co–C(8)	60.3(4)	Co–C(10)–O(4)	174(1)
Pt–Co–C(9)	131.3(7)		

The molecular structure of complex **3** was also determined by X-ray diffraction analysis. The atomic coordinates are listed in Table 9, an ORTEP drawing is given in Fig. 4 and selected bond distances and angles are listed in Table 10. The co-ordination around the platinum is distorted square planar, but the Co–Pt–C(1) angle is considerably bent [164.3(5)°]. The plane of the phenyl group is almost perpendicular to the co-ordination plane of the platinum. The co-ordination around the cobalt is similar to that in **2**, except that one of the carbonyl ligands [C(8)–O(2)] shows remarkable interaction with the platinum atom. The short Pt–C(8) distance [2.41(1) Å], the small Pt–Co–C(8) angle [60.3(4)°] and the bent Co–C(8)–O(2) bond [165(1)°] indicate a bent semibridging character of the carbonyl ligand.[23] This also accounts for the non-linearity of the Co–Pt–C(1) bond. It should be pointed out that complex **3** undergoes no further ligand migration as in **1**, but its structure corresponds to that of the intermediate species in the formation of **1** from [PtPh(O$_3$SCF$_3$)(PPh$_3$)$_2$] and [Co(CO)$_4$]$^-$. It is also interesting that insertion of CO into the metal–phenyl bond did not occur in the case of complex **3** even under CO (see below). Yamamoto and co-workers[25] recently reported that the reactivity of a cationic platinum complex [PtR(PMe$_3$)$_2$(solvent)]$^+$ toward insertion of CO is much lower than that of the palladium analogue, and this is in accordance with our observation that complex **3**, but not the corresponding benzoyl complex analogous to **2**, was formed exclusively.

Reaction of Complex **3** *with* L (CO, PMe$_3$ *or* Bu^{t}NC).—Reactions of complex **3** with L = CO, PMe$_3$ or Bu^{t}NC were monitored by ^{31}P-{^{1}H} NMR, IR and electroconductivity measurements. Addition of 1 equivalent of PMe$_3$ or Bu^{t}NC to **3** in thf caused instantaneous disappearance of the red colour of **3**. Even at −70 °C the reaction of **3** and Bu^{t}NC was completed within a few seconds. Introduction of CO into a thf solution of **3** also resulted in a fading of the colour, but in this case it did not disappear completely. The ^{31}P-{^{1}H} NMR spectra of the reaction mixtures obtained from the treatment of **3** with PMe$_3$, Bu^{t}NC and CO showed signals assignable to [PtPh(PMe$_3$)$_3$]$^+$ {[^{2}H$_8$]thf, −50 °C, δ −27.2 [t, ^1J(Pt–P) 1708, ^2J(P–P) 23] and −17.6 [d, ^1J(Pt–P) 2515, ^2J(P–P) 23 Hz]},[26] *trans*-[PtPh(PMe$_3$)$_2$(CNBu^t)]$^+$ {[^{2}H$_8$]thf, δ −18.3 [s, ^1J(Pt–P) 2439 Hz]} and *trans*-[PtPh(PMe$_3$)$_2$(CO)]$^+$ {[^{2}H$_8$]thf, δ −15.4 [s, ^1J(Pt–P) 2438 Hz]}, respectively. In each case, the IR spectra revealed the formation of [Co(CO)$_4$]$^-$ [ν(CO) 1887 cm^{-1} in thf]. In addition, a ν(CO) (2097 cm^{-1}) or ν(NC) (2197 cm^{-1}) absorption assignable to *trans*-[PtPh(PMe$_3$)$_2$L]$^+$ (L = CO or Bu^{t}NC) was observed. The electroconductivity measurements showed a drastic increase in molar conductance (0.18 S cm^2 mol^{-1} for **3**, 17–31 S cm^2 mol^{-1} after the reaction with CO, PMe$_3$ or Bu^{t}NC), indicating that heterolytic cleavage of the Pt–Co bond occurred on reaction with L. These observations clearly showed that L attacks the platinum to give ionic complexes *trans*-[PtPh(PMe$_3$)$_2$L][Co(CO)$_4$].

Such heterolytic cleavage was observed for some d^8 organometallic complexes.[20,27] In contrast, complexes **1** and **2** did not show any such reactivity, and interestingly, **3** in benzene failed to react with CO, PMe$_3$ or Bu^{t}NC.

Thermolysis of Complexes **1b** *and* **1c** *and Mechanism of Palladium-catalysed Formation of* [Co(OCR)(CO)$_3$(PPh$_3$)].—Complexes **1b** and **1c** did not decompose in C$_6$D$_6$ under nitrogen at 50 °C. However, thermolysis in C$_6$D$_6$ under a carbon monoxide atmosphere at 50 °C for 3 h gave [Co(C$_6$H$_4$Me-4)(CO)$_3$(PPh$_3$)] (47%) and [Co(OCMe)(CO)$_3$(PPh$_3$)] (52%), respectively (^{1}H NMR spectroscopy). In contrast, **2** decomposed in C$_6$D$_6$ under nitrogen at 50 °C,

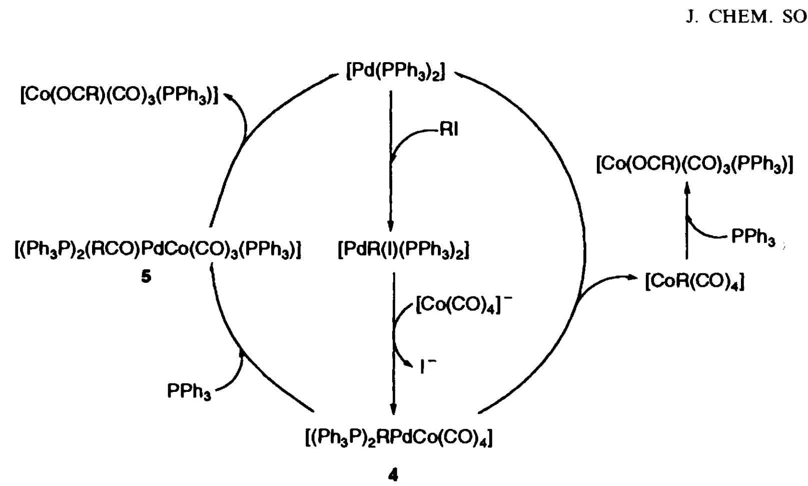

Scheme 2

however the resulting solution showed many signals in the $^{31}P-\{^1H\}$ NMR spectrum and attempts to isolate the products were unsuccessful. Complex **2** did not react in C_6D_6 under a carbon monoxide atmosphere at 50 °C. Complex **3** did not show any spectral change at 50 °C under nitrogen or CO. The results of the thermolysis of **1b** and **1c** unambiguously indicate the involvement of a Pd–Co dinuclear species similar to **1** as a key intermediate in the catalytic reaction.

On the basis of these observations, we propose a catalytic mechanism as depicted in Scheme 2. The oxidative addition of RI to Pd^0 and the substitution of the iodo ligand with $[Co(CO)_4]^-$ forms a Pd–Co dinuclear intermediate **4**, which is considered to correspond to complex **3**. The reaction of **4** with PPh_3 added to the reaction system would give a dinuclear benzoyl complex **5** through the migration of a CO ligand from cobalt to palladium followed by migratory insertion of the CO ligand into the R–Pd bond.[28] The reductive elimination from the palladium centre of **5** yields $[Co(OCR)(CO)_3(PPh_3)]$ and regenerates the palladium(0) species. Alternatively, intermediate complex **4** may undergo reductive elimination to give $[CoR(CO)_4]$ which further reacts with PPh_3 to produce $[Co(OCR)(CO)_3(PPh_3)]$ as the final product.[18]

By this study we have shown that the transfer of an organic group from one metal centre to another in a heterometallic complex plays a critical role in the catalytic transformation of RI, $K[Co(CO)_4]$ and PPh_3 to $[Co(OCR)(CO)_3(PPh_3)]$. It also constitutes an important part of the Pd–Co-catalysed carbonylation of RI.[5]

References

1 D. A. Roberts and G. L. Geoffroy, in *Comprehensive Organometallic Chemistry*, eds. G. Wilkinson, F. G. A. Stone and E. W. Abel, Pergamon, Oxford, 1982, vol. 6, pp. 763–877; B. D. Dombek, *Organometallics*, 1985, **4**, 1707; P. Braunstein and J. Rose, in *Stereochemistry of Organometallic and Inorganic Compounds*, ed. I. Bernal, Elsevier, Amsterdam, 1989, vol. 3, pp. 3–138; G. Süss-Fink and G. Meister, *Adv. Organomet. Chem.*, 1993, **35**, 41; M. E. Broussard, B. Juma, S. G. Train, W.-J. Peng, S. A. Laneman and G. G. Stanley, *Science*, 1993, **260**, 1784; R. D. Adams, T. S. Barnard, Z. Li, W. Wu and J. H. Yamamoto, *J. Am. Chem. Soc.*, 1994, **116**, 9103.

2 M. Hidai, A. Fukuoka, Y. Koyasu and Y. Uchida, *J. Mol. Catal.*, 1986, **35**, 29; M. Hidai and H. Matsuzaka, *Polyhedron*, 1988, **7**, 2369; Y. Ishii, M. Sato, H. Matsuzaka and M. Hidai, *J. Mol. Catal.*, 1989, **54**, L13.

3 Y. Misumi, Y. Ishii and M. Hidai, *J. Mol. Catal.*, 1993, **78**, 1.

4 Y. Misumi, Y. Ishii and M. Hidai, *Chem. Lett.*, 1994, 695.

5 Y. Misumi, Y. Ishii and M. Hidai, *Organometallics*, 1995, **14**, 1770.

6 G. A. Artamkina, A. Yu. Mil'chenko, N. A. Bumagin, I. P. Beletskaya and O. A. Reutov, *Metalloorg. Khim.*, 1988, **1**, 34; *Organomet. Chem. USSR*, 1988, **1**, 17.

7 D. R. Coulson, *Inorg. Synth.*, 1972, **13**, 121.

8 W. F. Edgell and J. Lyford, IV, *Inorg. Chem.*, 1970, **9**, 1932.

9 P. Fitton, M. P. Johnson and J. E. McKeon, *Chem. Commun.*, 1968, 6.

10 N. Kawata, T. Mizoroki and A. Ozaki, *Bull. Chem. Soc. Jpn.*, 1974, **47**, 1807.

11 J. Chatt and B. L. Shaw, *J. Chem. Soc.*, 1959, 705.

12 G. Calvin and G. E. Coates, *J. Chem. Soc.*, 1960, 2008.

13 J. Chatt and B. L. Shaw, *J. Chem. Soc.*, 1959, 4020.

14 M. Ferrer, O. Rossell, M. Seco and P. Braunstein, *J. Chem. Soc., Dalton Trans.*, 1989, 379.

15 J. D. Ruddick and B. L. Shaw, *J. Chem. Soc. A*, 1969, 2801.

16 TEXSAN Crystal Structure Analysis Package, Molecular Structure Corporation, Houston, TX, 1985 and 1992.

17 C. K. Johnson, ORTEP II, Report ORNL-5138, Oak Ridge National Laboratory, Oak Ridge, TN, 1976.

18 R. F. Heck and D. S. Breslow, *J. Am. Chem. Soc.*, 1962, **84**, 2499.

19 R. E. Dessy, R. L. Pohl and R. B. King, *J. Am. Chem. Soc.*, 1966, **88**, 5121.

20 A. Fukuoka, T. Sadashima, I. Endo, N. Ohashi, Y. Kambara, T. Sugiura, K. Miki and S. Komiya, *Organometallics*, 1994, **13**, 4033.

21 J. K. Stille, in *The Chemistry of the Metal–Carbon Bond*, eds. F. R. Hartley and S. Patai, Wiley, Chichester, 1985, vol. 2, p. 763.

22 See for example, R. Bender, P. Braunstein, J. Fischer, L. Ricard and A. Mitschler, *Nouv. J. Chem.*, 1981, **5**, 81; P. Braunstein, J. Dehand and J. F. Nenning, *J. Organomet. Chem.*, 1975, **92**, 117; J. P. Barbier, P. Braunstein, J. Fischer and L. Ricard, *Inorg. Chim. Acta*, 1978, **31**, L361.

23 R. H. Crabtree and M. Lavin, *Inorg. Chem.*, 1986, **25**, 805; C. Q. Simpson, II and M. B. Hall, *J. Am. Chem. Soc.*, 1992, **114**, 1641.

24 G. Le Borgne, S. E. Bouaoud, D. Grandjean, P. Braunstein, J. Dehand and M. Pfeffer, *J. Organomet. Chem.*, 1977, **136**, 375.

25 Y. Kayaki, F. Kawataka, I. Shimizu and A. Yamamoto, The 30th International Conference on Co-ordination Chemistry, Kyoto, July 24–29, 1994, Abstracts, p. 233.

26 W. Lin, S. R. Wilson and G. S. Girolami, *Inorg. Chem.*, 1994, **33**, 2265.

27 H. C. Clark and J. D. Ruddick, *Inorg. Chem.*, 1970, **9**, 1226; K. A. Hooton, *J. Chem. Soc. A*, 1970, 1896; S. Komiya and J. K. Kochi, *J. Am. Chem. Soc.*, 1976, **98**, 7599; P. Braunstein, C. de Méric de Bellefon and M. Ries, *Inorg. Chem.*, 1988, **27**, 1338.

28 K. Kudo, M. Hidai and Y. Uchida, *J. Organomet. Chem.*, 1971, **33**, 393.

Received 10*th April* 1995; *Paper* 5/02307F